Supporting Information for

Rational Design of Dibenzothiophene-S,S-dioxide-Containing Conjugated Polymers for Highly Efficient Photosynthesis of Hydrogen Peroxide in Pure Water

Jun Wu, Qi Zhang, Feng Wang*

School of Chemical Engineering and Pharmacy, Wuhan Institute of Technology, Wuhan 430205, People's Republic of China

*Corresponding Author: psfwang@wit.edu.cn

Section 1. Experimental methods

Materials

3,7-Bis(4,4,5,5-tetramethyl-1,3,2-dioxaborolan-2-yl)dibenzothiophene-S,S-dioxide (M1) were synthesized according to the procedure in our previous report.[1] 1,4-dibromobenzene (M2), 2,5-dibromopyridine (M3), 2,5-dibromopyrazine (M4) and other reagents were purchased from Aladdin Reagent Co., Ltd and used without further purification.

Synthesis of PSO-B. The polymer was synthesized by Suzuki−Miyaura coupling reaction under argon atmosphere. M1 (468 mg, 1 mmol), M2 (236 mg, 1 mmol), $Pd(PPh_3)_4$ (5 mg) and DMF (25 mL) were added into a round bottom flask. After degassing by bubbling with argon for 30 min, Na_2CO_3 aqueous solution (2 M, 3 mL) was added to the mixture. The solution was heated to 140 ℃ and stirred for 72 h. The precipitate was obtained by filtration, and washed thoroughly with methanol and water, respectively. Soxhlet extraction was used for further impurity removal. The product was dried by freeze-drying (yield: 90.2%). Anal. calcd for ($C_{18}H_{12}O_2S$) (%): C 74.34; H 3.64; O 11.00; S 11.02. Found: C 69.99; H 3.77; O 15.94; S 10.30. The residual Pd content is 0.05 wt% from inductively coupled plasma-mass spectrometry (ICP-MS) measurement.

Synthesis of PSO-BN1. PSO-BN1 was prepared by using the same procedure as PSO-B and the yield was 87.2%. Anal. calcd for ($C_{17}H_{11}NO_2S$) (%): C 69.97; H 3.28; O 10.96; S 10.99; N 4.80. Found: C 67.35; H 3.55; O 14.67; S 9.61; N 4.82. The residual Pd content is 0.04 wt% from ICP-MS measurement.

Synthesis of PSO-BN2. PSO-BN2 was prepared by using the same procedure as PSO-B and the yield was 89%. Anal. calcd for ($C_{16}H_{10}N_2O_2S$) (%): C 64.77; H 3.64; O 11.00; S 11.02; N 9.57. Found: C 64.63; H 3.25; O 14.00; S 10.07; N 8.05. The residual Pd content is 0.04 wt% from ICP-MS measurement.

Characterization

Thermogravimetric analysis (TGA) was tested by Q500 over the temperature ranging from 30 to 700 °C at a heating rate of 10 °C min^{-1} under N_2 atmosphere. X-ray diffractometer (DX-2700) was utilized to measure the powder X-ray diffraction (XRD) of polymers. Fourier transform infrared (FTIR) spectrum was collected on Bruker FTIR spectrometer. Elemental analysis (EA, Thermo Scientific Flash 2000) was tested to determine the content of C, S, H, N and O elements. The morphology and element mapping were obtained on the field-emission scanning electron microscopy (SEM, Hitachi JSM-7001F). The content of residual palladium was determined by inductively coupled plasma (ICP-MS, Agilent 7700(MS)). Solid-state ^{13}C NMR measurement was carried out on a Bruker 600M spectrometer at a MAS rate of 10 kHz. The absorption of three polymers under solid state was analyzed by UV–vis diffuse reflectance spectra (UV-2600, Shimadzu). $BaSO_4$ was used as the reflection standard. Photoluminescence (PL, Hitachi F-7100) spectra were measured under excitation wavelength at 365 nm. Time-resolved photoluminescence (TRPL) spectra were measured on Edinburgh Instruments FLS 980 fluorescence spectrophotometer. X-ray photoelectron spectroscopy (XPS) was conducted on an EscaLab Xi system (Thermo Scientific) equipped with an Al Kα microfocused as X-ray source. The XPS spectra were

calibrated with a peak position of 284.8 eV for C 1s. The surface potential of the polymers in darkness and under irradiation was tested by the atomic force microscopy with Kelvin probe force microscopy (KPFM) mode (SPM-9700, Shimadzu). In situ diffuse reflectance infrared Fourier transform spectroscopy was conducted on Bruker TENSOR II. Zeta potential and particle size was carried out on Malvern Zetasize Nano-ZS90. The concentration of the suspension was 0.05 g L^{-1}.

Electrochemical analysis

Cyclic voltammetry (CV), transient photocurrent response and electrochemical impedance spectroscopy (EIS) were measured by a three-electrode cell system on CHI-660E electrochemical workstation. Platinum, Ag/AgCl electrode and glassy carbon is used as the counter electrodes, the reference electrode and the working electrode, respectively. The transient photocurrent response uses 0.5 mol L^{-1} Na_2SO_4 solution as the electrolyte. EIS uses a mixture solution with potassium ferricyanide, potassium ferricyanide and potassium chloride as the electrolyte.

CV was performed in acetonitrile solution of 0.1 mol L^{-1} MBu4NPF6, using ferrocene/ferrocene (Fc/Fc^+) as reference with the absolute energy was −4.8 eV (vs. vacuum). The highest occupied molecular orbital (HOMO) energy levels and lowest unoccupied molecular (LUMO) energy levels were calculated by the following equation:

$$E_{\mathrm{HOMO}} = -e(E_{ox} + 4.8 - E_{1/2(Fc/Fc^+)}) \text{ (eV)} \quad \text{(S1)}$$

$$E_{\mathrm{LUMO}} = -e(E_{red} + 4.8 - E_{1/2(Fc/Fc^+)}) \text{ (eV)} \quad \text{(S2)}$$

where E_{red} and E_{ox} are the onsets of the reduction and oxidation potential.

Electron paramagnetic resonance (EPR) measurement

EPR was acquired using an EPR spectrometer (Bruker EMXplus-6/1) with 5,5-dimethyl-1-pyrroline-N-oxide (DMPO) as the spin trap. The suspension was prepared as follows: 5 mg samples dispersed in 5 mL weakly alkaline solution (pH=8), and 20 μL DMPO (50 mM) mixed within the suspension. The suspension was transferred into a cylindrical quartz cell, degassed by argon for 15 min, and then irradiated under a 300 W Xe lamp (λ ＞420 nm) for 10 min. Afterward, the signals of DMPO−·OH were tested on an EPR spectrometer.

The DMPO−·O_2^- signal test was performed in the same procedure as that of the DMPO−·OH signal. O_2 was continuously bubbled into the suspension for 15 min. The suspensions were transferred into a cylindrical quartz cell and irradiated under a 300 W Xe lamp (λ ＞420 nm) for 10 min.

Photocatalytic experiments

Typically, 5 mg photocatalysts was dispersed in 50 mL deionized water by ultrasonication. No other sacrificial reagents or co-catalysts were added. The reaction suspension was stirred for 15 min in dark to achieve the adsorption and desorption equilibrium under air atmosphere. The pH value was adjust using 0.1 mol L^{-1} NaOH or 0.1 mol L^{-1} H_2SO_4 aqueous solution. The photocatalytic H_2O_2 production experiment was irradiated with a 300 W Xe lamp (Beijing Perfectlight, PLS-SXE300D) equipped with a $\lambda \geq 420$ nm filter (307.9 mW cm^{-2}) at ambient temperature. After the photocatalytic reaction, the concentration of H_2O_2 were detected by iodometry method.

H_2O_2 detection methods

The method of detecting the concentration of H_2O_2 is as follows. After the photocatalytic reaction, 1 mL of the filtrate which was obtained by filtering with 0.22 μm filter membrane mixed with 1 mL aqueous solution of potassium hydrogen phthalate (0.1 mol L^{-1}) and 1 mL aqueous solution of potassium iodide (0.4 mol L^{-1}). In the presence of H^+, the reaction between H_2O_2 with I^- occurs to generate triiodide anions (I_3^-) (Equation S3), which shows a characteristic absorption peak at about 350 nm. Moreover, the amount of generated H_2O_2 was estimated the following calibration curve.[2]

$$H_2O_2 + 3I^- + 2H^+ \rightarrow I_3^- + 2H_2O \quad \text{(S3)}$$

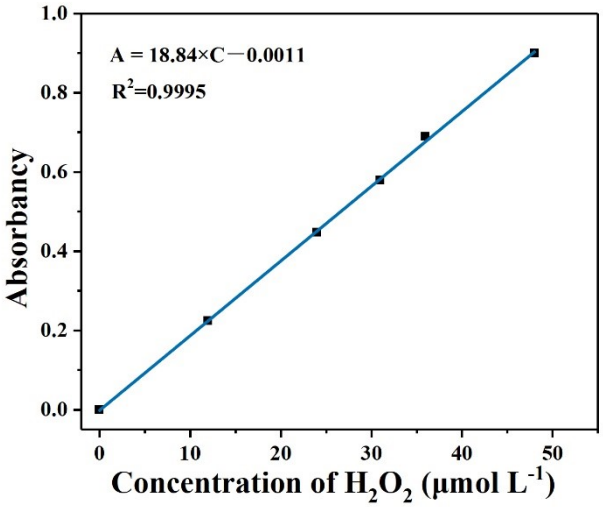

The calibration curve of the relationship between the H_2O_2 concentration with the absorbance of I_3^-.

Apparent quantum yield (AQY) measurement

AQY of PSO-BN2 for H_2O_2 production was carried out using 300 W Xe lamp with band pass filter. The light intensities at 420, 475, 500 and 550 nm were 23.5, 27.8, 31.3 and 39.7 mW cm^{-2}, respectively. The AQY was calculated using the equation below:

$$AQY\ (\%) = \frac{2 \times Number\ of\ evolved\ H_2O_2\ molecules}{Number\ of\ incident\ photons} \times 100\%$$
$$= \frac{2 \times C \times N_A}{S \times P \times t \times \lambda/(h \times c)} \times 100\% \quad \text{(S4)}$$

Where C is the amount of H_2O_2 production (μmol); N_A is the Avogadro constant (6.02×10^{23} mol^{-1}); S is the irradiation area (cm^2); P is monochromatic light intensity (W cm^{-2}); t is the irradiation time (s); λ is the monochromatic light wavelength (nm); h is the Planck constant (6.626×10^{-34} J·s); c is the velocity of light in vacuum (3×10^8 m s^{-1}).

The solar-to-chemical conversion (SCC) efficiency was determined by using AM 1.5 solar simulator as light source. The SCC was calculated by the following equation:

$$\text{SCC}\ (\%) = \frac{\Delta G(H_2O_2) \times n(H_2O_2)}{I_{AM} \times S_{ir} \times t_{ir}} \times 100\% \quad \text{(S5)}$$

$\Delta G(H_2O_2)$=117 J/mol, I_{AM} is the light intensity (358 mW cm^{-2}), S_{ir} is the irradiation area (6.25 cm^2).

Photocatalytic O_2 evolution tests

PSO-BN2 (5 mg) were ultrasonically dispersed into 50 mL $AgNO_3$ aqueous solution (0.5 mol L^{-1}), then stirred for 15 min in darkness after removing O_2 by vacuum extraction. O_2 evolution tests were conducted by a Labsolar-6A circulation system (Beijing Perfectlight Technology Co., Ltd). The suspension was irradiated with a 300 W Xe lamp with an optical filter ($\lambda \geq 420$ nm) at ambient temperature. The O_2 formation was estimated by online gas chromatograph (GC9790 II, Fuli).

Computational details

The optimization and frequency combined with vertical excitation properties were

carried out at the wb97xd/6-311g(d) level in the Gaussian 09 program. Two repetition models were optimized to represent the major surface properties of PSO-B, PSO-BN1 and PSO-BN2.

The adsorption energy of O_2 (E_{ads}) was computed by:

$$E_{ads} = E_{tot} - E_{sub} - E_{O_2} \quad \text{(S6)}$$

where E_{tot} is the calculated total energy of the adsorption system, E_{sub} is the calculated energy of the polymer substrate, and E_{O_2} is the calculated energy of the O_2.

For analysis of the molecular planarity, Multiwfn Ver. 3.8 (dev) was performed.[3]

Section 2. Supplementary Figures and Tables

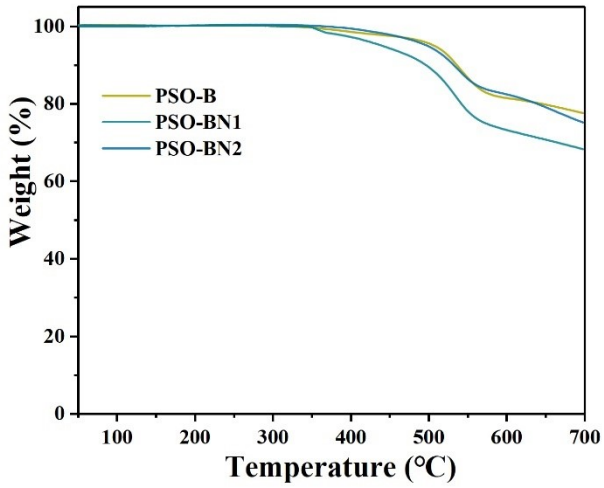

Figure S1. TGA of the three polymers under N_2 atmosphere.

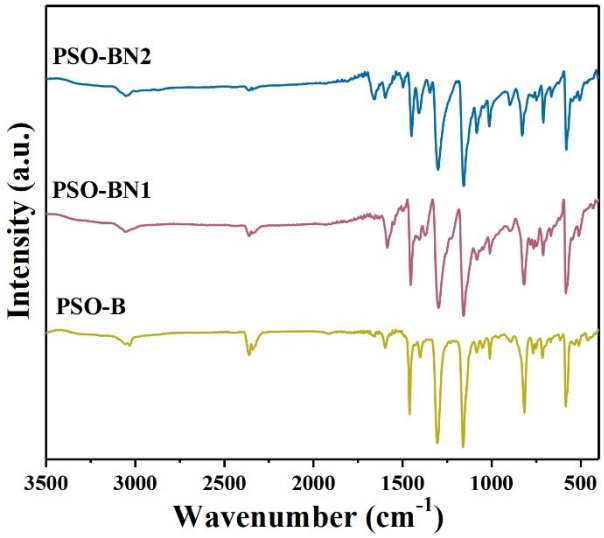

Figure S2. FTIR spectra of the three polymers.

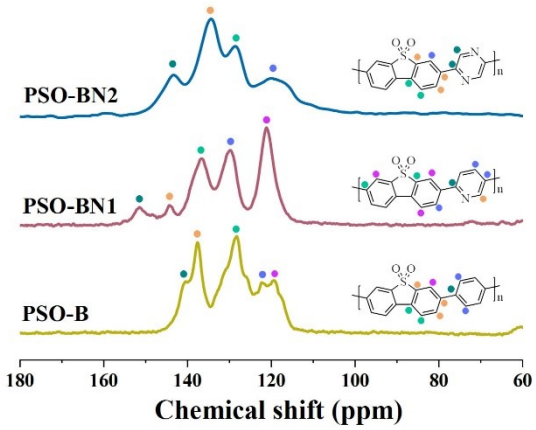

Figure S3. Solid-state ^{13}C NMR spectra of the three polymers.

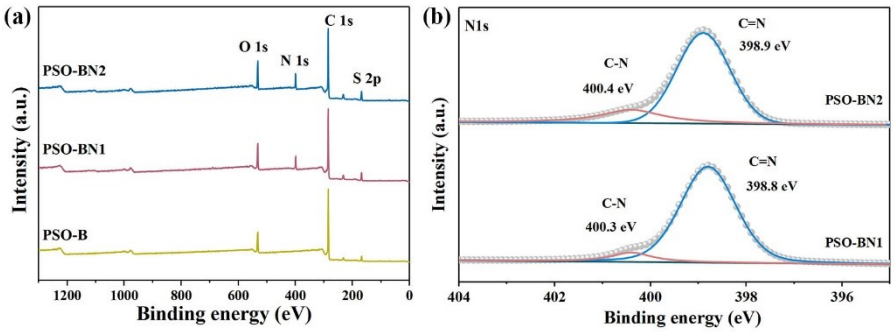

Figure S4. (a) XPS survey spectra and (b) high-resolution XPS of N 1s spectra of the polymers.

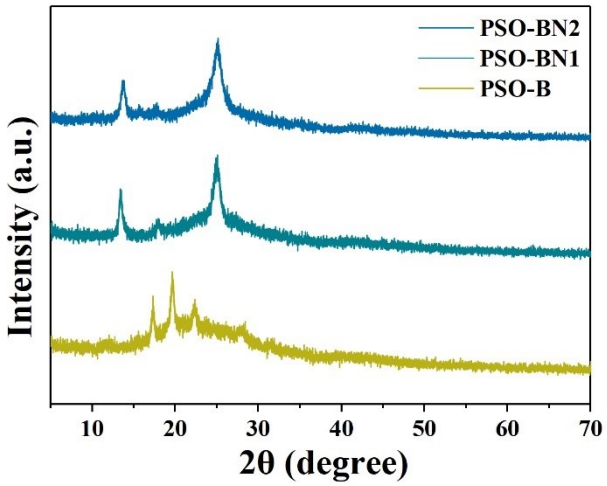

Figure S5. XRD patterns of the three polymers.

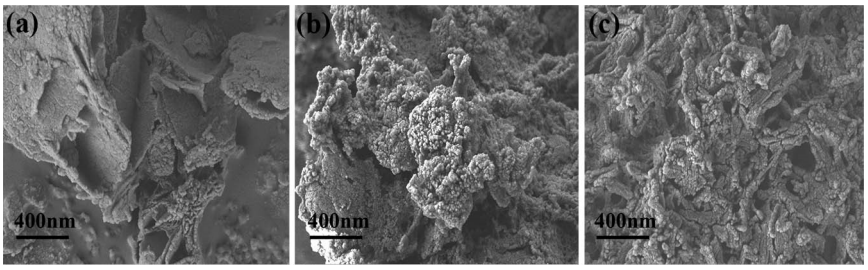

Figure S6. SEM images of (a) PSO-B, (b) PSO-BN1, (c) PSO-BN2.

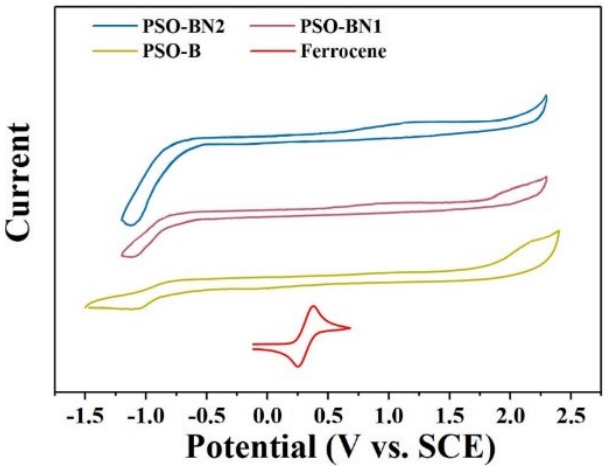

Figure S7. CV curves of the three polymers.

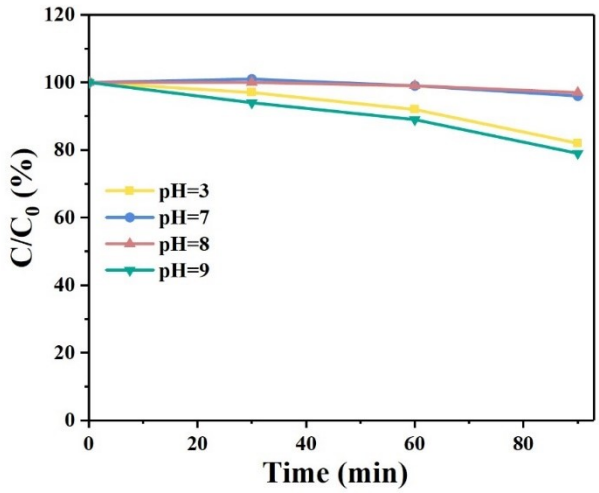

Figure S8. The photocatalytic decomposition of H_2O_2 over PSO-BN2 in aqueous solution with different pH values. (Experiment conditions: 5 mg PSO-BN2, 50 mL H_2O_2 aqueous solution with different pH values)

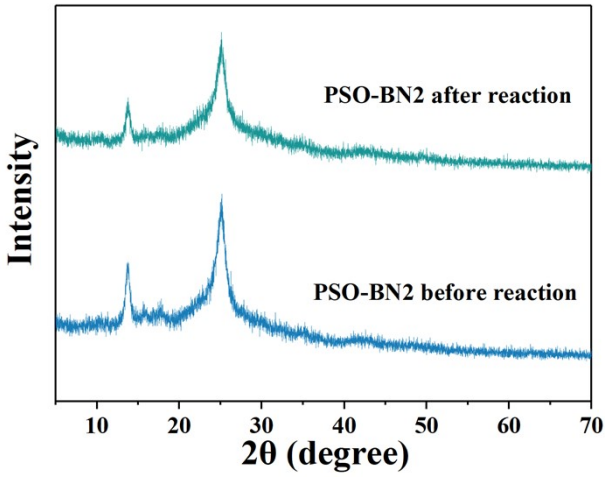

Figure S9. XRD patterns of PSO-BN2 before and after the photocatalytic reaction.

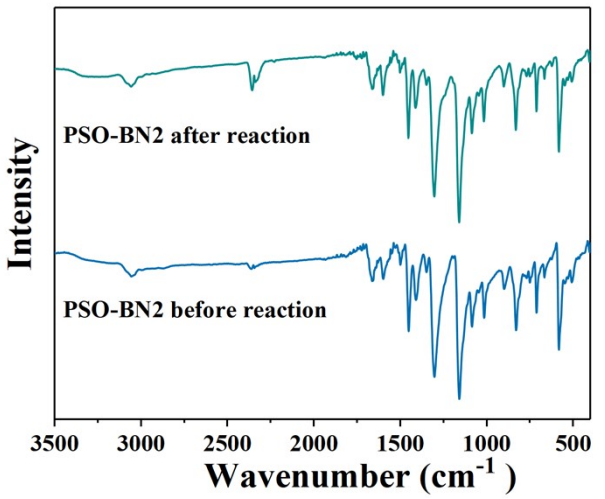

Figure S10. FTIR spectra of PSO-BN2 before and after the photocatalytic reaction.

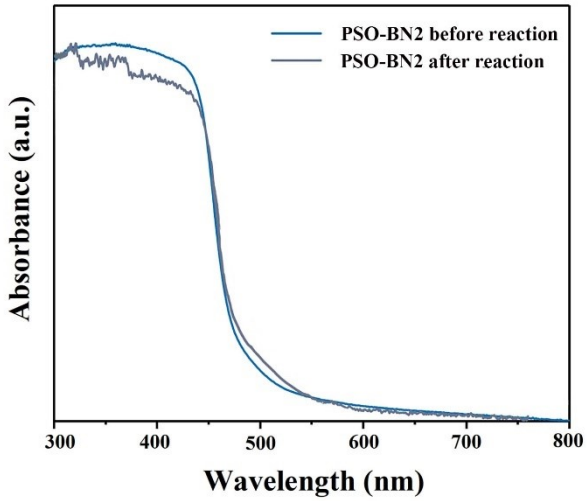

Figure S11. UV–vis diffuse reflectance spectra of PSO-BN2 before and after the photocatalytic reaction.

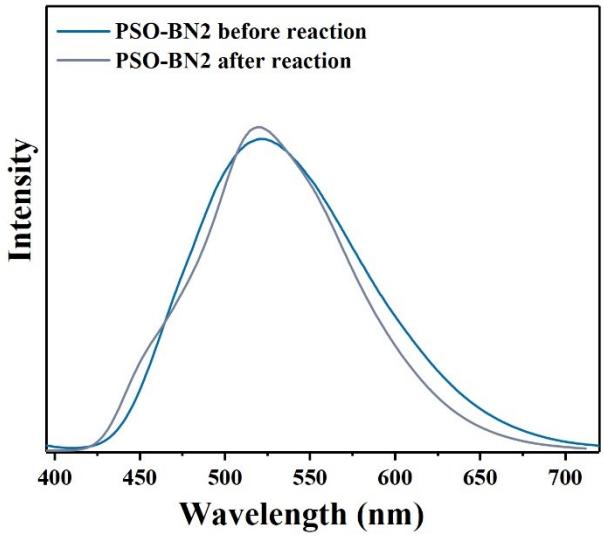

Figure S12. PL spectra of PSO-BN2 before and after the photocatalytic reaction.

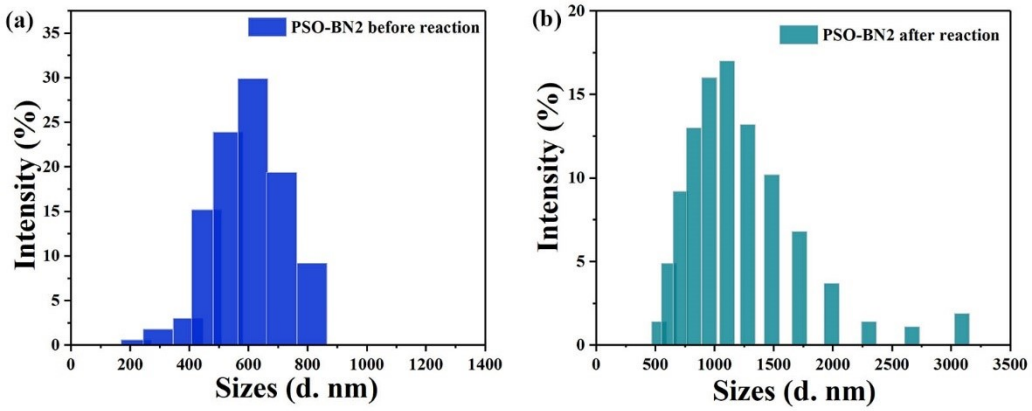

Figure S13. DLS measurements of PSO-BN2 before and after the photocatalytic reaction.

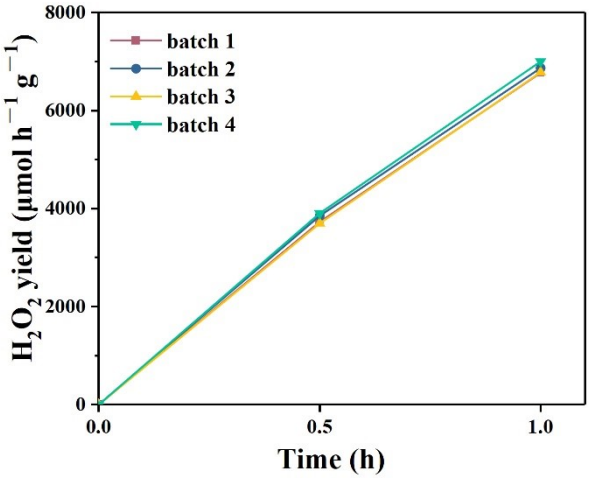

Figure S14. H_2O_2 generation of PSO-BN2 over different batches.

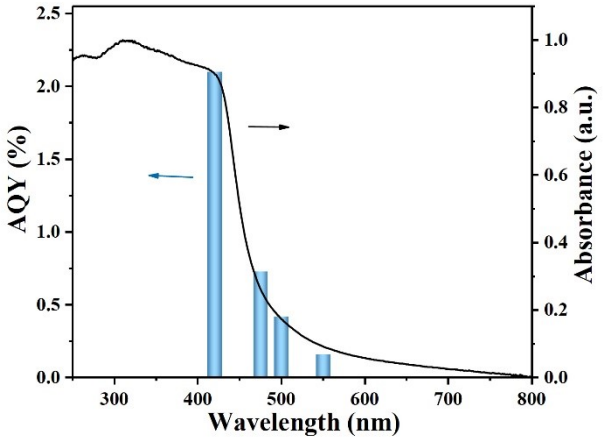

Figure S15. Wavelength dependence of AQY for photocatalytic H_2O_2 generation of PSO-BN2.

Figure S16. Water contact angles of PSO-B, PSO-BN1 and PSO-BN2.

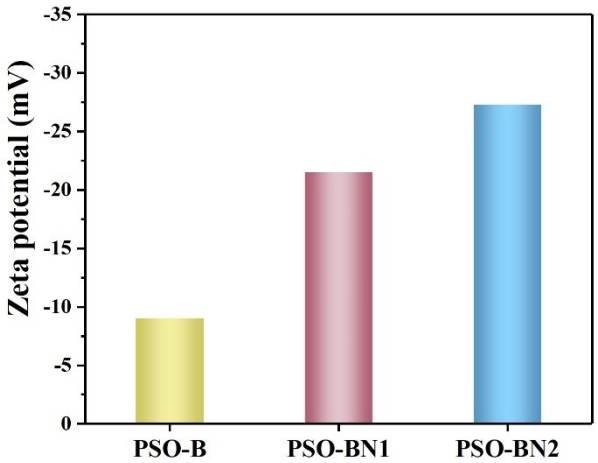

Figure S17. Zeta potential of PSO-B, PSO-BN1 and PSO-BN2 in water.

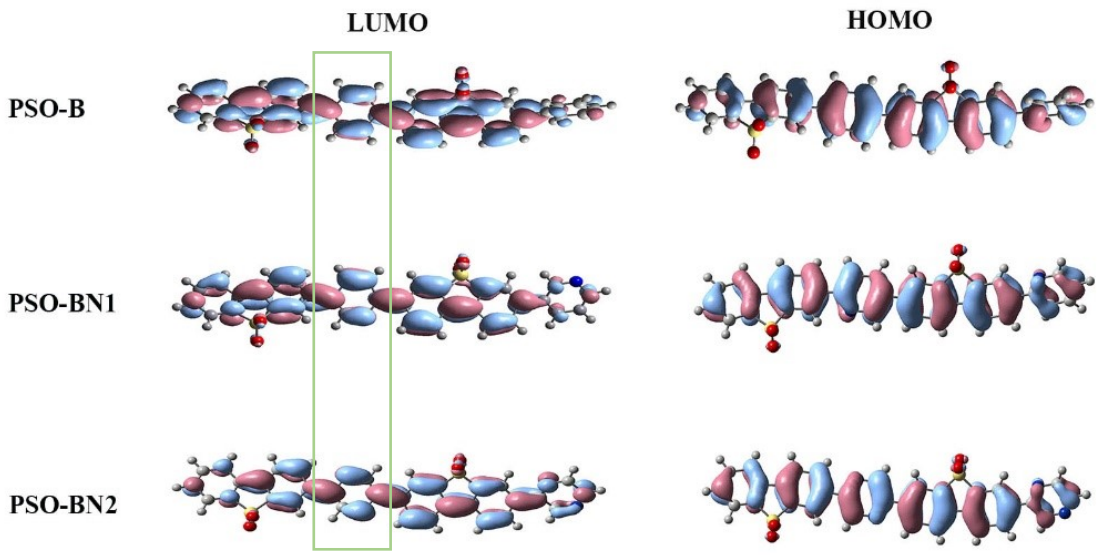

Figure S18. The HOMO and LUMO orbital distribution of the three polymers.

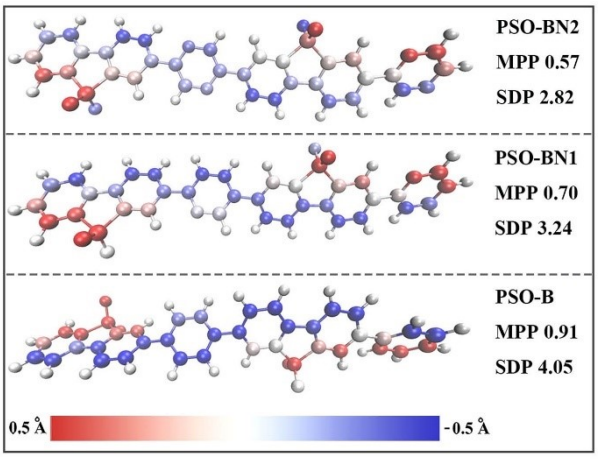

Figure S19. MPP and SDP values of the three polymers. The bluer (redder) the color, the larger the distance of the atom below (above) the fitting plane.

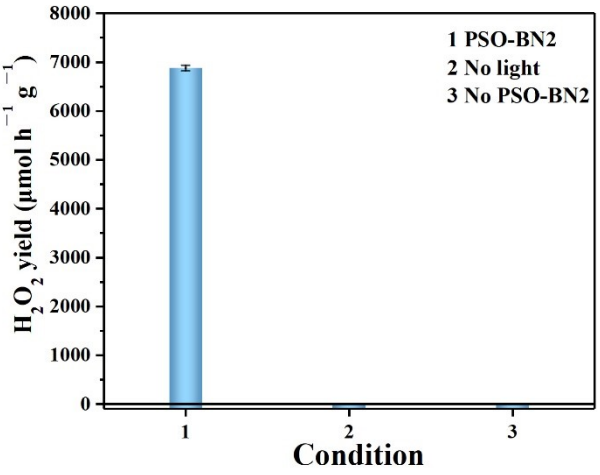

Figure S20. The H_2O_2 yield under different experimental conditions.

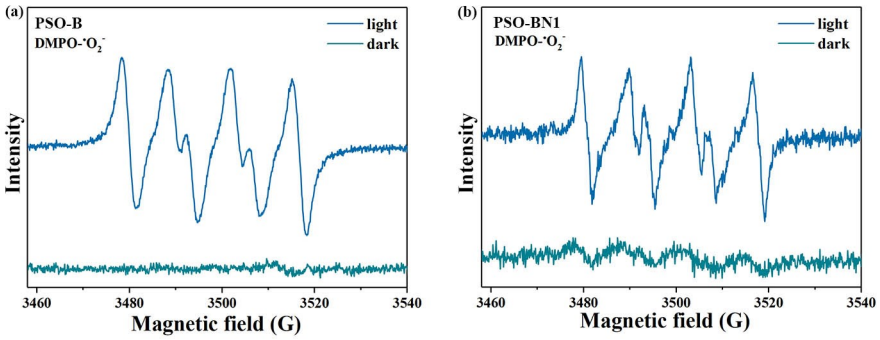

Figure S21. EPR spectra of DMPO-·O_2^- for (a) PSO-B and (b) PSO-BN1.

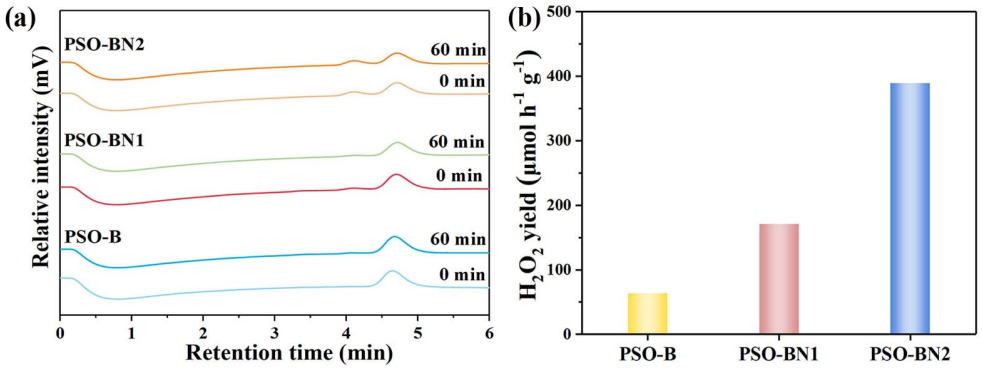

Figure S22. (a) Photocatalytic O_2 evolution performance of the three polymers. (b) The H_2O_2 yield over the three polymers in $AgNO_3$ aqueous solution under vacuum.

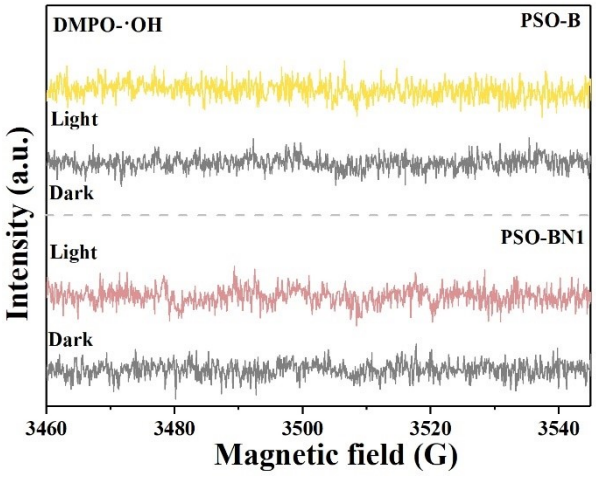

Figure S23. EPR spectra of DMPO-·OH over PSO-B and PSO-BN1.

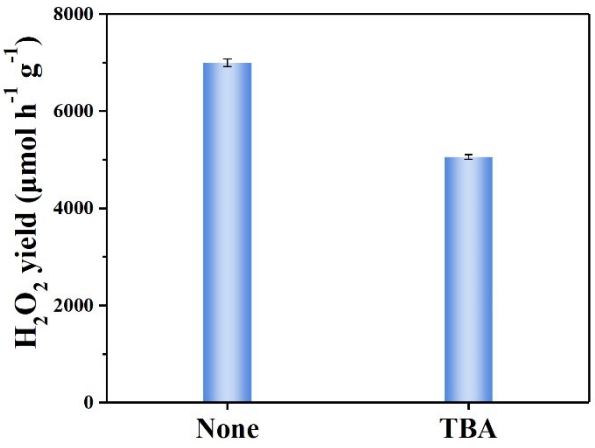

Figure S24. Photocatalytic H_2O_2 production of PSO-BN2 in the presence of TBA. (Experimental conditions: 5 mg photocatalyst, 50 mL H_2O (pH=8), 0.5 mol L^{-1} TBA)

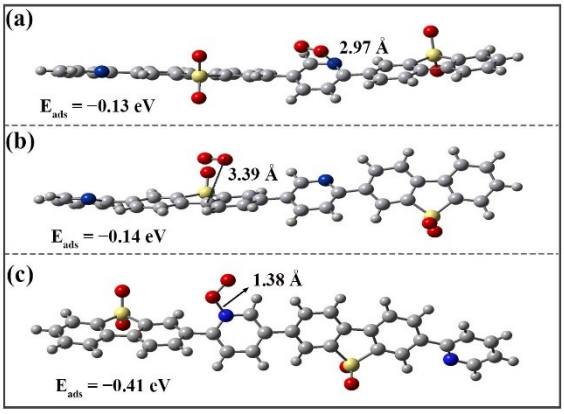

Figure S25. O_2 adsorption on different components in PSO-BN1 (a) pyridine ring, (b) SO moiety and (c) N atom. (C and H: light gray; N: blue; O: red; S: yellow).

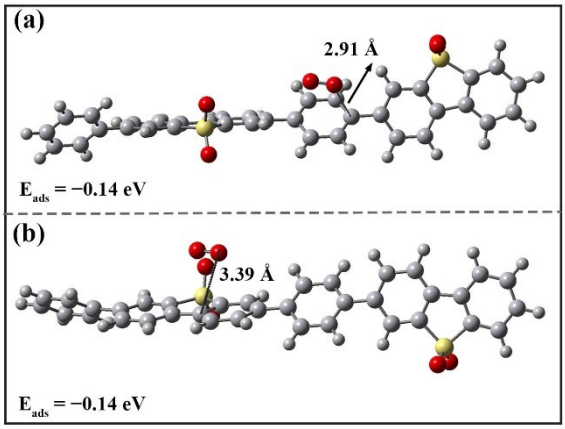

Figure S26. O_2 adsorption on different components in PSO-B (a) benzene ring, (b) SO moiety (C and H: light gray; N: blue; O: red; S: yellow).

Table S1. Summary of band energy of PSO-B, PSO-BN1, PSO-BN2.

Polymers	Reduction Potential (V)	Oxidation Potential (V)	E_{LUMO}[a)] (eV)	E_{HOMO}[a)] (eV)	E_{LUMO}[b)] (v)	E_{HOMO}[b)] (V)
PSO-B	−0.74	1.83	−3.74	−6.31	−0.76	1.81
PSO-BN1	−0.71	1.96	−3.77	−6.44	−0.73	1.94
PSO-BN2	−0.67	2.05	−3.81	−6.53	−0.69	2.03

[a)] E vs. vacuum (eV); [b)] E vs. NHE (V).

Table S2. Comparison of the reaction conditions and photocatalytic H_2O_2 production performance without sacrificial reagent.

Materials	H_2O_2 yield[a)] (μmol h^{-1} g^{-1})	Light (nm)	Mass (mg)	H_2O (mL)	Ref.
PSO-BN2	6996	λ ⩾420	5	50	This work
TPT	3214	λ >400	1	50	[4]
RF-DHAQ	1820	λ >420	10	50	[5]
TTF	2760	λ ⩾400	5	10	[6]
DBTP	10010	420⩽λ ⩽780	2	20	[7]
TpDz	7327	λ >420	3	18	[8]
Reduced g-C_3N_4	1700	λ >420	100	100	[9]
CQM-1	3676	420⩽λ ⩽700	10	15	[10]
NMT400	270.9	AM1.5G	20	50	[11]
CDA300	557.2	λ >420	10	40	[12]
$Bi_4O_5Br_2$/g-C_3N_4	2480	λ>420	50	50	[13]
ZIF-8	150	Full spectrum	50	100	[14]

MRF-250	582	λ>420	50	30	[15]
PtO_x-RGO-CN_x	275	λ>365	20	100	[16]
TPB	2900	λ>420	50	50	[17]
PC-MB-3	1385.42	λ ⩾420	50	20	[18]
SnO_2@g-C_3N_4	1021.15	λ ⩾420	20	20	[19]
Bpt-CTF	3268.1	-	10	50	[20]
CDs1-NCN	1938	420⩽λ ⩽700	10	15	[21]
PEI/C_3N_4	208.1	AM 1.5	20	20	[22]
Bpy-TAPT	4038	λ>420	5	30	[23]
FS-COFs	3904.3	λ>400	5	20	[24]
APFac	1123.5	λ>420	10	50	[25]
PCN	2063.21	λ>420	100	50	[26]
ATA	1119.2	λ>420	10	40	[27]
Ni_{SAPS}-PuCN	640.1	λ≥420	30	30	[28]

[a] H_2O_2 rate is more than 100 μmol h^{-1} g^{-1}

Table S3. Summary of PL lifetimes of PSO-B, PSO-BN1 and PSO-BN2.

Polymer	τ_1 [ns]	Rel [%]	τ_2 [ns]	Rel [%]	τ_3 [ns]	Rel [%]	T [ns]
PSO-B	0.62	42.28	2.81	38.67	11.98	19.05	2.76
PSO-BN1	0.85	24.83	2.60	66.94	9.91	8.23	3.63
PSO-BN2	0.76	33.25	2.92	49.27	12.10	17.48	3.81

References

1 Y. X. Liu, J. Wu and F. Wang, *Appl. Catal. B: Enviton.*, 2022, **307**, 121144.

2 N. V. Klassen, D. Marchington and H. C. E. McGowan, *Anal. Chem.*, 1994, **66**, 2921−2925.

3 T. Lu and F. W. Chen, *J. Comput. Chem.*, 2012, **33**, 580−592.

4 H. J. Yan, M. H. Shen, Y. Shen, X. D. Wang, W. Lin, J. H. Pan, J. He, Y. X. Ye, X. Yang, F. Zhu, J. Q. Xu, J. G. He and G. F. Ouyang, *Proc. Natl. Acad. Sci. U. S. A.*, 2022, **119**, 2202913119

5 C. Zhao, X. Y. Wang, Y. F. Yin, W. M. Tian, G. Zeng, H. T. Li, S. Ye, L. M. Wu and J. Liu, *Angew. Chem. Int. Edit.*, 2023, **62**, 2022183.

6 J. N. Chang, Q. Li, J. W. Shi, M. Zhang, L. Zhang, S. Li, Y. F. Chen, S. L. Li and Y. Q. Lan, *Angew. Chem. Int. Edit.*, 2023, **62**, 202218868.

7 G. Li, P. Fu, Q. Yue, F. Ma, X. Zhao, S. Dong, X. Han, Y. Zhou and J. Wang, *Chem Catalysis*, 2022, **2**, 1734−1747.

8 Q. Liao, Q. Sun, H. Xu, Y. Wang, Y. Xu, Z. Li, J. Hu, D. Wang, H. Li and K. Xi, *Angew. Chem. Int. Edit.* 2023, **62**, e202310556.

9 Z. D. Zhu, H. H. Pan, M. Murugananthan, J. Y. Gong and Y. R. Zhang, *Appl. Catal. B: Enviton.*, 2018, **232**, 19−25.

10 H. Shi, Q. Y. Wu, Z. Y. Wu, Y. Liu, X. T. Wang, H. Huang, Y. Liu and Z. H. Kang, *Catal. Sci. Technol.*, 2022, **12**, 1837−1842.

11 C. Yang, S. J. Wan, B. C. Zhu, J. G. Yu and S. W. Cao, *Angew. Chem. Int. Edit.*, 2022, **61**, 202208438.

12 C. C. Chu, Q. J. Li, W. Miao, H. H. Qin, X. R. Liu, D. C. Yao and S. Mao, *Appl. Catal. B: Enviton.*, 2022, **314**, 121485.

13 X. S. Zhao, Y. Y. You, S. B. Huang, Y. X. Wu, Y. Y. Ma, G. Zhang and Z. H. Zhang, *Appl. Catal. B: Enviton.*, 2020, **278**, 119251.

14 A. L. Chang, V. H. Nguyen, K. Y. A. Lin and C. C. Hu, *Arab. J. Chem.*, 2020, **13**, 8301−8308.

15 L. Yuan, C. Q. Zhang, J. Wang, C. Liu and C. Z. Yu, *Nano Res.*, 2021, **14**, 3267−3273.

16 D. Liu, J. N. Shen, Y. Y. Xie, C. W. Qiu, Z. Z. Zhang, J. L. Long, H. X. Lin and X. X. Wang, *ACS Sustain. Chem. Eng.*, 2021, **9**, 6380−6389.

17 L. J. Li, L. P. Xu, Z. F. Hu and J. C. Yu, *Adv. Funct. Mater.*, 2021, **31**, 2106120.

18 Q. Y. Wu, Y. Liu, J. J. Cao, Y. Sun, F. Liao, Y. Liu, H. Huang, M. W. Shao and Z. H. Kang, *J. Mater. Chem. A*, 2020, **8**, 11773−11780.

19 M. He, X. Zhang, S. J. Song, J. S. Yao, Z. Fang, W. W. Wang, X. L. Yuan, C. Y.

Li, H. Li, P. G. Li, W. Y. Song and Z. X. Li, *ACS Sustain. Chem. Eng.*, 2022, **10**, 4494−4503.

20 C. B. Wu, Z. Y. Teng, C. Yang, F. S. Chen, H. Bin Yang, L. Wang, H. X. Xu, B. Liu, G. F. Zheng and Q. Han, *Adv. Mater.*, 2022, **34**, 2110266.

21 K. Q. Wei, H. D. Nie, Y. Li, X. Wang, Y. Liu, Y. J. Zhao, H. Shi, H. Huang, Y. Liu and Z. H. Kang, *J. Colloid Interface Sci.*, 2022, **616**, 769−780.

22 X. K. Zeng, Y. Liu, Y. Kang, Q. Y. Li, Y. Xia, Y. L. Zhu, H. L. Hou, M. H. Uddin, T. R. Gengenbach, D. H. Xia, C. H. Sun, D. T. McCarthy, A. Deletic, J. G. Yu and X. W. Zhang, *ACS Catal.*, 2020, **10**, 3697−3706.

23 Y. Liu, W. K. Han, W. W. Chi, Y. Q. Mao, Y. Q. Jiang, X. D. Yan and Z. G. Gu, *Appl. Catal. B: Enviton.*, 2023, **331**, 122691.

24 Y. Luo, B. P. Zhang, C. C. Liu, D. H. Xia, X. W. Ou, Y. P. Cai, Y. Zhou, J. Jiang and B. Han, *Angew. Chem. Int. Edit.*, 2023, **62**, 202305355.

25 X. Y. Wang, X. W. Yang, C. Zhao, Y. T. Pi, X. B. Li, Z. F. Jia, S. Zhou, J. J. Zhao, L. M. Wu and J. Liu, *Angew. Chem. Int. Edit.*, 2023, **62**, 202302829.

26 S. Yan, Y. Li, X. Yang, X. Jia, J. Xu and H. Song, *Adv. Mater.*, 2023, 2307967.

27 C. Chu, D. Yao, Z. Chen, X. Liu, Q. Huang, Q. Li and S. Mao, *Small*, 2023, **19**, 2303796.

28 X. Zhang, H. Su, P. Cui, Y. Cao, Z. Teng, Q. Zhang, Y. Wang, Y. Feng, R. Feng, J. Hou, X. Zhou, P. Ma, H. Hu, K. Wang, C. Wang, L. Gan, Y. Zhao, Q. Liu, T. Zhang

and K. Zheng, *Nat. Commun.*, 2023, **14**, 7115.